Supraglacial ponds regulate runoff from Himalayan debris-covered glaciers

Irvine-Fynn, Tristram; Porter, Philip R.; Rowan, Ann Victoria; Quincey, Duncan J.; Gibson, Morgan; Bridge, Jonathan W.; Watson, C. Scott; Glasser, Neil

Published in:
Geophysical Research Letters

DOI:
10.1002/2017GL075398

Publication date:
2017

Citation for published version (APA):
Irvine-Fynn, T., Porter, P. R., Rowan, A. V., Quincey, D. J., Gibson, M., Bridge, J. W., Watson, C. S., & Glasser, N. (2017). Supraglacial ponds regulate runoff from Himalayan debris-covered glaciers. *Geophysical Research Letters*, *44*(23), 11894-11904. https://doi.org/10.1002/2017GL075398

Geophysical Research Letters

RESEARCH LETTER
10.1002/2017GL075398

Key Points:
- The monsoon season runoff hydrograph from Khumbu Glacier displays progressive changes in diurnal timing and recession characteristics
- We propose that observed hydrological behavior results from seasonal evolution of supraglacial ponds and connections
- Predicted expansion of debris-covered areas and pond extents will influence downstream timing, availability, and quality of meltwater in the Himalaya

Supporting Information:
- Supporting Information S1

Correspondence to:
T. D. L. Irvine-Fynn,
tdi@aber.ac.uk

Citation:
Irvine-Fynn, T. D. L., Porter, P. R., Rowan, A. V., Quincey, D. J., Gibson, M. J., Bridge, J. W., … Glasser, N. F. (2017). Supraglacial ponds regulate runoff from Himalayan debris-covered glaciers. *Geophysical Research Letters*, *44*, 11,894–11,904. https://doi.org/10.1002/2017GL075398

Received 21 AUG 2017
Accepted 19 NOV 2017
Accepted article online 29 NOV 2017
Published online 11 DEC 2017

Supraglacial Ponds Regulate Runoff From Himalayan Debris-Covered Glaciers

Tristram D. L. Irvine-Fynn[1], Philip R. Porter[2], Ann V. Rowan[3], Duncan J. Quincey[4], Morgan J. Gibson[1], Jonathan W. Bridge[5], C. Scott Watson[4], Alun Hubbard[1,6], and Neil F. Glasser[1]

[1]Centre for Glaciology, Department of Geography and Earth Sciences, Aberystwyth University, Aberystwyth, UK, [2]Department of Biological and Environmental Sciences, University of Hertfordshire, Hatfield, UK, [3]Department of Geography, University of Sheffield, Sheffield, UK, [4]School of Geography, University of Leeds, Leeds, UK, [5]Department of the Natural and Built Environment, Sheffield Hallam University, Sheffield, UK, [6]Centre for Arctic Gas Hydrate, Environment and Climate, Department of Geosciences, The Arctic University of Norway, Tromsø, Norway

Abstract Meltwater and runoff from glaciers in High Mountain Asia is a vital freshwater resource for one-fifth of the Earth's population. Between 13% and 36% of the region's glacierized areas exhibit surface debris cover and associated supraglacial ponds whose hydrological buffering roles remain unconstrained. We present a high-resolution meltwater hydrograph from the extensively debris-covered Khumbu Glacier, Nepal, spanning a 7 month period in 2014. Supraglacial ponds and accompanying debris cover modulate proglacial discharge by acting as transient and evolving reservoirs. Diurnally, the supraglacial pond system may store >23% of observed mean daily discharge, with mean recession constants ranging from 31 to 108 h. Given projections of increased debris cover and supraglacial pond extent across High Mountain Asia, we conclude that runoff regimes may become progressively buffered by the presence of supraglacial reservoirs. Incorporation of these processes is critical to improve predictions of the region's freshwater resource availability and cascading environmental effects downstream.

1. Introduction

An estimated 1.4 billion people depend on freshwater sourced from snow and ice melt in High Mountain Asia (Immerzeel et al., 2010). Although highly variable across the region, this meltwater typically contributes between 20% and 50% of the total annual runoff (Bookhagen & Burbank, 2010; Immerzeel & Bierkens, 2012; Lutz et al., 2014). Contemporary observations (Bolch et al., 2012; Brun et al., 2017; Kääb et al., 2012; Pritchard, 2017) and predicted trends (e.g., Shea, Immerzeel, et al., 2015; Soncini et al., 2016) of glaciers in the Himalaya demonstrate declining ice volumes but highlight uncertainty over the associated glacio-hydrological impacts and consequent water stress arising from climate change. One important cause of this ambiguity is the presence of a supraglacial debris mantle present on many of the region's glaciers, which covers up to 36% of the glacierized area in the Everest region (Bolch et al., 2012; Kääb et al., 2012; Scherler et al., 2011; Thakuri et al., 2014). This debris mantle commonly causes downglacier ablation areas to exhibit low surface gradients and velocities (e.g., Quincey et al., 2007; Salerno et al., 2017; Scherler et al., 2011; Thompson et al., 2016), and its overall extent is increasing and predicted to expand further (Bolch et al., 2008; Rowan et al., 2015; Thakuri et al., 2014). Supraglacial debris exerts a critical influence on glacier response to climate forcing because, dependent on its thickness, debris can either accelerate or retard ablation (Evatt et al., 2015; Østrem, 1959). This effect, coupled with the dynamic topography of the glacier surface, promotes highly heterogenous ablation and the formation of surface lakes and ponds, which are a common feature of receding debris-covered glaciers (Basnett et al., 2013; Benn et al., 2012; Gardelle et al., 2011; Miles et al., 2016, Miles, Willis, et al., 2017, Miles, Steiner, et al., 2017; Narama et al., 2017; Reynolds, 2000; Watson et al., 2016). However, the processes and causal relationships underpinning the spatial distribution of supraglacial ponds remain unclear (Salerno et al., 2017).

Supraglacial ponds are "hotspots" of glacier ablation (Mertes et al., 2017) due to their reflective and thermal characteristics (Benn et al., 2001; Miles et al., 2016; Sakai et al., 2000; Watson, Quincey, Carrivick, & Smith, 2017) and the presence of bare-ice cliffs associated with pond formation and growth (Sakai et al., 2002; Brun et al., 2016; Watson, Quincey, Carrivick, & Smith, 2017). Consequently, ponds may accelerate glacier thinning and recession and act as temporary meltwater storage reservoirs (Benn et al., 2001, 2012). Ponds on debris-covered glaciers are commonly either transient features due to inception or collapse of near-surface or shallow englacial drainage routes and consequent drainage, or appear "perched" in closed basins where efficient flow paths are absent (Benn et al., 2001; Miles, Steiner, et al., 2017; Reynolds, 2000; Watson, Quincey, Carrivick, Smith, Rowan, et al., 2017). Seasonally, ponds on Himalayan glaciers typically grow both in area and depth (Watson, Quincey, Carrivick, Smith, Rowan, et al., 2017), attaining maximum extent mid-monsoon and declining in size thereafter (Miles, Willis, et al., 2017; Narama et al., 2017; Watson et al., 2016). Interannually, debris redistribution and change in surface topography result in variation in pond positions (Narama et al., 2017; Watson et al., 2016), and as ponds attain their local hydrological base level, they may evolve into larger scale lakes (Thompson et al., 2016; Mertes et al., 2017). Observations of supraglacial pond water quality confirm that hydrological linkages do exist between ponds (Bhatt et al., 2016; Takeuchi et al., 2012), and pond extent may be governed by the evolving development and (re)organization of supraglacial drainage systems (Miles, Steiner, et al., 2017; Watson et al., 2016, Watson, Quincey, Carrivick, Smith, Rowan, et al., 2017). Yet the extent to which these ponds impact upon meltwater generation and modify the seasonal hydrograph remains poorly quantified.

A lack of in situ observations of meltwater generation, transit, and runoff for Himalayan glaciers (Bajracharya et al., 2015; Immerzeel et al., 2012) has led to uncertainties in the prediction of their hydrological response to environmental forcing. For example, some numerical models of debris-covered glacier systems utilize a linear reservoir parameterization linking proglacial discharge to meltwater production (e.g., Fujita & Sakai, 2014; Ragettli et al., 2015). Such methods though fail to account for the potential hydrological complexities in the region. Specifically, the presence of interconnected supraglacial ponds implies a potentially complex hydrological system (Miles, Steiner, et al., 2017) that will modulate the water inputs to and outputs from the glacier system. Hence, the acquisition of detailed measurements characterizing the hydrological behavior of debris-covered glaciers on diurnal to seasonal time scales is an imperative for improved predictions of meltwater delivery to downstream water resources throughout the Himalaya. Here we present the results of a glacier-scale runoff monitoring program at the debris-covered Khumbu Glacier in the Everest region of Nepal. Our measurements span a 190 day period from April to November 2014 including the summer monsoon season.

2. Field Site and Methods

Khumbu Glacier (27.97°N, 86.83°E) flows from the southern flanks of Mount Everest to its terminus at ~4,900 m above sea level (asl) (Figure 1a). The terminus elevation is slightly lower than the local permafrost limit of ~5,000 m asl (Schmid et al., 2015). The glacier is likely to be polythermal, with an estimated 17 m deep cold surface ice layer (Mae et al., 1975). The glacier thinned at approximately -0.6 m a^{-1} between 2000 and 2015, with losses of -1.4 m a^{-1} at elevations of 5,200–5,300 m asl (King et al., 2017). Approximately 47% of the 41 km^2 glacier including the Changri Nup and Changri Shar tributaries is debris-covered (Figure 1b). Supraglacial debris thickness varies from 0.1 m to over 3 m and is concentrated over the lowermost 8 km of the glacier (Soncini et al., 2016), overlying 20 m to 440 m of glacier ice (Gades et al., 2000). Recent observations (e.g., Nuimura et al., 2011) indicate that this debris cover has become increasingly topographically uneven: differential ablation has resulted in a complex glacier surface characterized by the presence of numerous supraglacial water bodies (Watson et al., 2016; Wessels et al., 2002). Throughout 2014, ~1% of the total debris-covered area comprised supraglacial ponds (Figures 1b–1e). However, as elsewhere in the region, the hydrological evolution and connectivity of these supraglacial ponds is poorly constrained. The Changri Nup and Changri Shar tributaries are now physically disconnected but retain a surface hydrological connection with the Khumbu Glacier tongue (Vincent et al., 2016). The only visible source of meltwater runoff flowing from the Khumbu catchment emerges from a turbid supraglacial lake situated close to the eastern glacier margin (Figure 1c). There is no evidence for any other active terminal or lateral outlets for englacial or subglacial drainage pathways. Runoff data were recorded immediately downstream of this outlet lake, where meltwater drains via a breach in the eastern Little Ice Age lateral moraine to the upper Dudh Koshi.

Discharge (*Q*) data were collected between 14 May and 13 November (day of year (DOY) 134 to 317) using standard methods (Herschy, 1995). A hydrological monitoring station was established in a stable reach of the sole outflow channel at 4930 m asl. Average water stage was recorded at 30 min intervals using a Druck PDCR1730 pressure transducer and Campbell Scientific (CS) CR1000 data logger. A stage-discharge rating curve was developed using triplicate dilutions (Hudson & Fraser, 2005) of 3 mL aliquots of 10% fluorescein

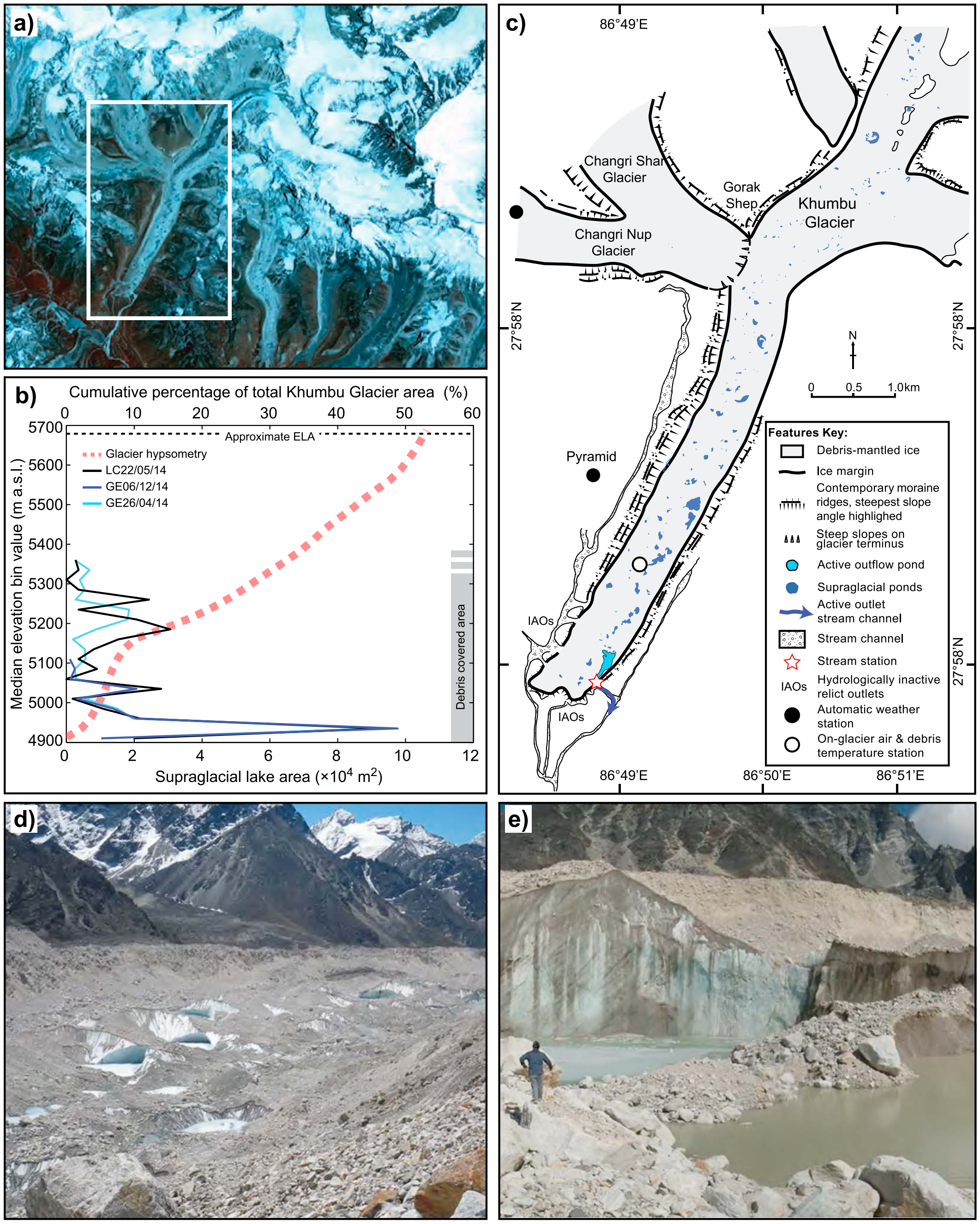

Figure 1. (a) ASTER imagery (September 2012) of the Everest region, Nepal, outlining lower elevations of the Khumbu Glacier; (b) hypsometry and supraglacial pond area in Khumbu Glacier ablation zone based on satellite imagery from 26 April, 22 May, and 6 December 2014 (see Watson et al., 2016); (c) ablation zone of Khumbu Glacier highlighting key data collection sites and major geomorphological features, including hydrologically inactive outlets (IAOs) indicative of abandoned drainage routes and supraglacial lake positions on 26 April 2014 prior to the onset of the monsoon season; (d and e) oblique images illustrating typical debris cover and pond morphology, taken during the pre-monsoon period, May 2014.

and a Turner Designs Cyclops7 fluorometer linked to a CS CR10X data logger. A nonlinear stage-discharge relationship yielded a coefficient of determination of r^2 = 0.79 (n = 18). Estimated uncertainty in Q is <15%, although this is increased for higher Q values (see supporting information; Di Baldassarre & Montanari, 2009; Rantz et al., 1982; Sakai et al., 1997). On-glacier air temperature (T_a) and debris temperature (T_d) were monitored at 4,935 m asl using Gemini TinyTag2 logging thermistors with a stated measurement accuracy of ±0.4°C (Figure 1c). The T_a sensor was mounted in a naturally aspirated radiation shield 1 m above the debris surface; the T_d sensors were located within the debris layer at depths of 0.55 and 1.0 m below the surface and away from the debris-ice interface. All temperature measurements were recorded at 30 min intervals. Local incident shortwave radiation (SW_{in}) was recorded at an automatic weather station 5,363 m asl on the Changri Nup Glacier (Figure 1c) using a Kipp & Zonen CNR4 sensor with 3% uncertainty. Precipitation (*P*) was measured at Pyramid Observatory (Figure 1c) at 5,035 m asl using a Geonor T-200 gauge; these hourly data were corrected for undercatch of solid precipitation and have an estimated accuracy of ±15% (Sherpa et al., 2017).

We examined the timing of peak discharge and the shape of the diurnal hydrograph using standard approaches; lag times between time series were identified using a moving window cross correlation (e.g., Jobard & Dzikowski, 2006), while we classified diurnal hydrographs using a paired principal component analysis (PCA) and hierarchical cluster analysis (HCA) approach (e.g., Hannah et al., 2000; Swift et al., 2005). Specifically, daily (24 h) hydrographs were assumed to commence at low *Q* at 06:00, PCA was conducted without rotation, and only components with eigenvalues >1.0 were retained. PCA identified modes of diurnal *Q* variation defined by the standardized component loadings, and these loadings for each day were clustered using Euclidean distance measures and a within-groups linkage method. A total of six groups were identified and further classified using a second, independent HCA that defined diurnal hydrograph similarity based on key discharge metrics following *z*-score normalization. Daily hydrographs were then described based on "shape" defined by PCA clusters and "magnitude" identified in the secondary HCA.

Estimates of recession storage constants (*K*) for each diurnal hydrograph were derived from semilogarithmic plots of *Q* versus time (e.g., Gurnell, 1993; Hodgkins et al., 2013) where:

$$K = \frac{-t}{\ln\left(\frac{Q_t}{Q_0}\right)} \tag{1}$$

for which *t* is time since the start of the recession segment and Q_0 and Q_t the discharge at the start of the recession segment and at time *t*, respectively. For all days classified as exhibiting diurnal discharge cycles ($n = 117$) or constant recessional hydrographs ($n = 29$), *K*-values were calculated from the time step following peak discharge, or from 18:00 in the case of persistent recession hydrographs. Recession segments and associated aggregate recession constants were identified using segmented linear regression for cases exhibiting durations >1 h.

3. Results

The meteorological and discharge time series (Figures 2a–2d) for the 2014 monsoon season reveal that T_a and SW_{in} exhibited strong diurnal variations, with highest incident energy fluxes between 10:00 and 15:00, as typifies the region (see Shea, Wagnon, et al., 2015). These two variables were highly correlated over the diurnal cycle ($r > 0.5$, $p < 0.05$) throughout the observation period (Figure 2e). Seasonal changes in T_d aligned well with T_a, although at the daily time step, correlation suggested a changing lag between variables (Figure 2e). Despite a distinct diurnal variability in T_d, variation was suppressed at depth (Figure 2b), and T_d remained below 0°C following DOY 300. The seasonal pattern of Q broadly followed that of T_a with an underlying diurnal fluctuation of between 0.005 and 12.3 $m^3\ s^{-1}$ and daily mean *Q* peaking at ~9 $m^3\ s^{-1}$ that compares well with published records of discharge during 2014 for the upper Dudh Koshi (Soncini et al., 2016; see supporting information). Interestingly, diurnal correlation indicated that *Q* and both T_a and SW_{in} vary out of phase for much of the observation period (Figure 2e). *Q* lagged T_a progressively decreasing from 12 to 6 h until DOY 220 and subsequently returning to lags >12 h until DOY 285 when lags dropped again to ~6 h (Figure 2f). The diurnal hydrograph cycle became steadily delayed until DOY270 when T_d declined to ~5°C and continued to fall when a protracted hydrograph recession dominated. While statistically significant diurnal correlations between *Q* and *P* were found, these were inconsistent and showed no systematic trend (Figure 2e). Lag analysis highlighted statistically significant correlations ($r > 0.405$, $p < 0.05$) between *Q* and *P* over 24 h periods, predominantly with *Q* lagged by >10 h; however, no pattern in lag time was observed.

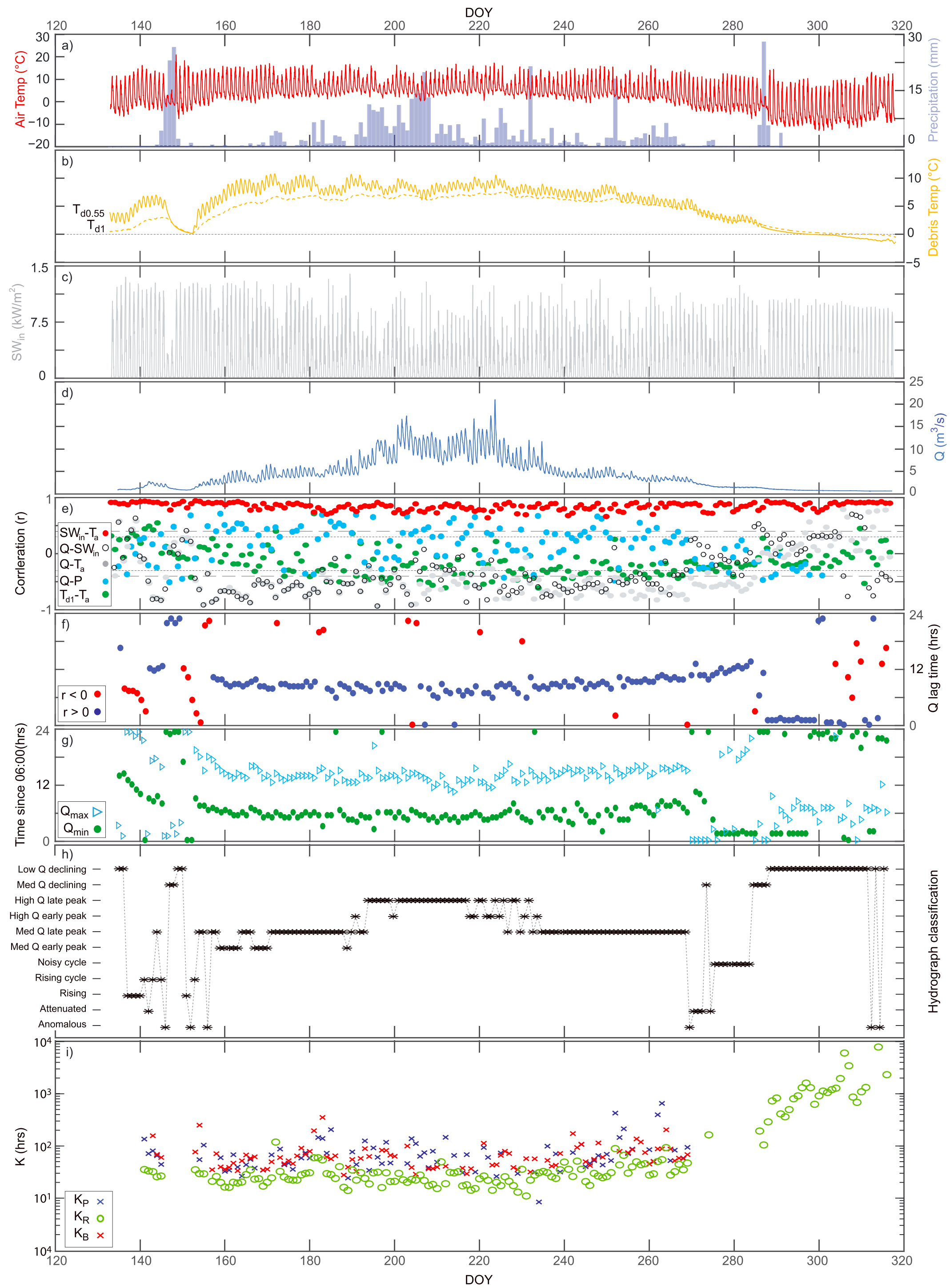

Figure 2. Time series of (a) on-glacier air temperature T_a and total daily precipitation P, (b) debris temperature T_d at 0.55 and 1.0 m below the debris surface, (c) incident shortwave radiation SW_{in}, and (d) meltwater discharge Q. Analyses identify (e) daily correlations between T_a, SW_{in}, P, and Q with the 95% confidence levels indicated for the hourly ($r \approx 0.41$) and half-hourly ($r \approx 0.29$) data sets, (f) the lag time between daily peak T_a and maximum Q, (g) the timing of minimum and maximum Q, (h) the daily hydrograph classification based on shape and magnitude, and (i) the three principal hydrograph recession constants (K_P, K_R, and K_B).

Three sequential recession segments were identified as typical within the time series: (i) slow decrease in Q lasting ≤7 h immediately following peak Q (K_P), (ii) major recession component of rapid decrease in Q over ~9 h duration (K_R), and (iii) a second slow decrease for ~5 h prior to the onset of the next diurnal cycle (K_B). Where only a singular extended recession was identified, this was taken to be K_R. K_P and K_B were found to be statistically similar but lacked a significant temporal trend, while K_R showed a strong nonlinear association with peak Q, decreasing and increasing as the monsoon season progressed. While aggregate K-values broadly agree with the magnitude of those identified in other glacial runoff records (mean K_P = 86.7 and K_B = 72.4 h, while mean K_R = 108 h for the season but 31.1 h before DOY270), the recession segment pattern contrasts with the commonly reported systematic increase in K-values over diurnal hydrograph recession segments (e.g., Gurnell, 1993; Hodgkins et al., 2013). No association between K-values and P or daily peak Q was found. In tests, uncertainty related to the rating curve used to derive the Q time series (see supporting information; Rantz et al., 1982) did not impact the recession patterns identified; however, if using a power law rating curve (Herschy, 1995), recession constants K_P, K_R, and K_B increased by 81 ± 30%, 51 ± 50%, and 57 ± 26% respectively.

4. Discussion

Our results from Khumbu Glacier indicate a hydrological configuration with both similarities and distinct differences to those typically reported for Alpine glacier systems in Europe and elsewhere. Systematic progression in timing of peak Q, seasonal undulation in diurnal discharge amplitude, diurnal hydrograph asymmetry, and clear patterns in hydrograph classification are commonly described for temperate, debris-free alpine glaciers (e.g., Hannah et al., 2000; Jobard & Dzikowski, 2006; Richards et al., 1996; Swift et al., 2005). Typically, as the snowline recedes upglacier and melt season advances, peak Q occurs progressively closer to the time of heightened SW_{in} and T_a and, even for large south-facing valley glaciers such as Aletschgletscher, equivalent in size to Khumbu Glacier, Q lags the meteorological drivers of melt by <5 h during much of the ablation season (e.g., Lang, 1973; Verbunt et al., 2003). As ablation continues on debris-free glaciers the amplitude of Q increases and the hydrograph form becomes more accentuated. Here particularly prior to DOY230 (Figures 3f–3h), the patterns of hydrograph characteristics resemble those reported for temperate alpine settings.

However, in contrast to debris-free alpine counterparts, the timing of daily peak and minimum discharge at Khumbu Glacier shows a more marked delay relative to meteorological drivers of ablation: peak Q occurs ≥6 h after maximum SW_{in} and T_a, while minimum Q commonly coincides with peak irradiance. Q lagging energy fluxes reflects the delay in energy transfers that initiate melt, particularly for those associated with exchange at the atmosphere-debris interface and through the debris layer (Carenzo et al., 2016) (Figure 2b). Further lags may relate to meltwater transit to the monitoring site. Transition in lag time between T_a and Q midseason is ascribed to changes in weather systems and lapse rates reported for the region during the monsoon (e.g., Shea, Wagnon, et al., 2015, Steiner & Pellicciotti, 2016), the reduction in both T_a and SW_{in}, and subtle changes in the hydrological function of the drainage system. The lack of association between Q and precipitation has been observed elsewhere on debris-covered glaciers (e.g., Thayyen et al., 2005). However, the elongated diurnal hydrograph recession diverges notably from other glacial observations, and more specifically, recession data reported here evidence neither "fast" supraglacial and "moderate" englacial and subglacial drainage flow paths, superimposed on a "slow" persistent base flow on a diurnal basis, nor a seasonal decline in recession storage constants (cf. Gurnell, 1993). Furthermore, the gauging station elevation (4,930 m asl) ensures the Q record solely relates to the supraglacial (debris-covered) and shallow englacial environment. Observations during 2014 confirmed that some supraglacial meltwaters entered a shallow englacial network, potentially allowing flow between supraglacial ponds, evidenced by spatial variability in pond turbidity that suggested hydrological connectivity (Figure 1e) (see Takeuchi et al., 2012). While geomorphic signatures suggested that meltwater that had once drained or followed seepage pathways through other moraine breach locations, contemporary field observations indicate that these are relict inactive features (IAOs: Figure 1c). Consequently, we discuss our data in the context of a conceptual model of the dominantly supraglacial drainage system illustrated in Figure 3, comprising a debris layer punctuated by a cascade of lakes or ponds.

The cascade of developing ponds represents a series of reservoirs capable of temporarily storing meltwater and delaying its transit downstream. Combining the pre-monsoon pond areas (~2.5×10^5 m^2; Figure 1) with

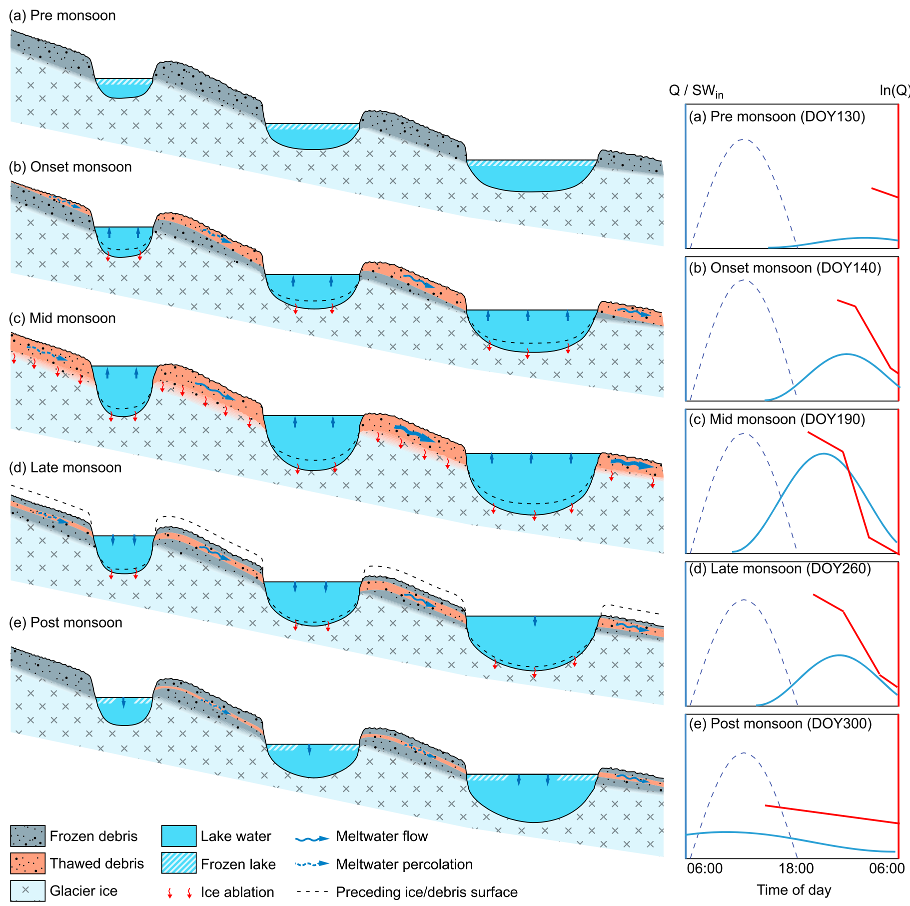

Figure 3. Conceptual model of the seasonal hydrological development of the surface of a Himalayan debris-covered glacier over an annual cycle. Indicative daily hydrometeorological plots for each stage are shown with SW_{in} (dashed), Q (blue), and a natural logarithmic transformed Q used to identify the recession components (red). (a) Pre-monsoon the surface is frozen following the winter period, (b) but as the monsoon season approaches, the debris-cover begins to thaw and water derived from melting intraclast ice and ponds commences flow and thermal ablation at the base of ponds. (c) Mid-monsoon the debris is fully thawed, ponds become connected and glacier ice melt occurs and ponds deepen through thermal ablation, which, coupled with monsoon rainfall, leads to more efficient drainage over the glacier ice surface. (d) Toward the end of the monsoon season the air temperatures drop and initiate freezing at the debris surface, while reductions in water flow facilitate upward freezing at the base of the debris layer; however, the thawed portion of the debris layer still transfers meltwater from ponds toward the glacier margin, albeit delayed. (e) Post-monsoon, which aligns with the latter portion of our records, continued freezeup of the lake and debris layer occurs restricting any transmission of meltwater as winter approaches and the glacier-wide hydrological system drains.

observation of the outflow lake level varying by ~0.7 m over a diurnal melt cycle, we estimate the supraglacial pond cascade on Khumbu Glacier to account for a minimum daily storage capacity of ~1.75×10^5 m^3 (equivalent to 23% of the observed mean daily discharge). Supported by evidence of progressive pond deepening during the monsoon season (e.g., Watson, Quincey, Carrivick, Smith, Rowan, et al., 2017), we conclude that the diurnal storage capacity of the pond system alone, not including the porous debris layer, can readily accommodate the observed daily mean P (~1.23×10^5 m^3 over the whole glacier area). The timing and magnitude of on-glacier storage may also be controlled by freeze-thaw processes, analogous to a periglacial environment given the local permafrost limit. During the winter, both the supraglacial debris layer and ponds are largely frozen, likely becoming impermeable and unable to convey any surface meltwater. As the monsoon season develops, the system progressively thaws (e.g., Benn et al., 2001; Miles et al., 2016; Narama et al., 2017; Sakai et al., 2000; Watson, Quincey, Carrivick, Smith, Rowan, et al., 2017). The ponds may become hydrologically linked by three key flow paths: those within the debris-covered mantle; shallow debris-filled crevasses (e.g., Benn et al., 2012; Gulley & Benn, 2007) or channels formed from collapsed near-surface englacial conduits (Miles, Steiner, et al., 2017); and debris- or water-choked near-surface passages (Watson, Quincey, Carrivick, Smith, Rowan, et al., 2017). Published figures for heterogeneous debris indicate permeability of between 10^{-2} and 10^{-6} m s^{-1} (Gulley & Benn, 2007; Muir et al., 2011; Parriaux & Nicoud, 1990; Woo & Steer, 1983), although mobilization of fines may further reduce hydraulic efficiency (Woo & Xia, 1995). When thawed, therefore, we anticipate the debris layer and associated supraglacial and shallow or collapsed englacial features may act as a depth-limited, transient storage reservoir, regulating bulk meltwater discharge over the glacier surface and between ponds and hence moderating the overall diurnal flow variance. The debris layer is underlain by glacier ice with discrete, spatially limited, shallow englacial flow paths analogous to continuous permafrost with isolated, closed talik. The result, in the monsoon-influenced climate, is a thermal regime dominated by the seasonal freezing and thawing of the debris layer, as is evident in our T_d time series, and for which the correlations between T_a and T_d (Figure 2e) likely reflect change in debris heat capacity with water content. Khumbu Glacier's supraglacial debris layer may therefore be considered equivalent to a seasonally cryotic active layer (Bonnaventure & Lamoureux, 2013).

As the monsoon season progresses, evolution of the debris mantle hydrological system may result in increased interpond connectivity. Progressive thaw at depth in the debris layer and glacier ice melt, despite enlarging the supraglacial storage capacity, also aids the development of increasingly efficient supra-permafrost drainage: interclast ice is replaced with water flow pathways and increased hydraulic permeability (Woo & Steer, 1983; Woo & Xia, 1995), providing more efficient connections through the debris and facilitating debris-ice interface and englacial flow path development (Gulley & Benn, 2007; Gulley et al., 2009; Miles, Steiner, et al., 2017; Watson, Quincey, Carrivick, Smith, Rowan, et al., 2017). Strengthening connectivity increases the rapidity of runoff through the cascading pond system. Sporadic activation, modification, or abandonment of flow paths and diurnal or seasonal variation in supraglacial pond storage capacity likely contributes to the observed variation of discharge recession (Figure 3i). Such delay, peak flow suppression, and attenuated recession, as seen in our data, are indicative of level-pool routing controlling meltwater transfer through a series of reservoirs (Montaldo et al., 2004) and, as such, the ponds may be conceptualized as thermokarst (Kirkbride, 1993).

Evidence for this role of supraglacial ponds and debris as regulators of meltwater discharge is exemplified by the diurnal hydrograph recession. When pond levels are at their peak or minima at seasonal and diurnal time scales, K_P and K_B are determined by the hydraulic conductivity of the (thawed) debris that separates the individual pond basins. K_P was not clearly associated with either T_a or SW_{in} nor with daily maximum discharge; the recession segment was not associated with the magnitude of meltwater production. Once daily meltwater provision declines or ceases, changes in hydraulic head drive drainage through the pond cascade and the major recession (K_R) is governed by outflow channel geometry rather than rates of inflow controlled by debris permeability. K_R remains broadly consistent over the hydrologically active period (DOY 134–270). Subsequently, particularly as T_a and T_d both fall and water drains from the pond cascade, water within the debris layer and debris-rich hydraulic connections between ponds refreezes, and the hydraulic efficiency of the system declines. This change is highlighted by $K_R > K_B$, the post-monsoon increase in K_R and a strongly negative, nonlinear relationship between K_R and peak Q.

The observations following DOY 230 of declining Q despite positive T_a and T_d and precipitation contributions are counterintuitive. However, given our hydrological analysis and conceptual model, it seems reasonable to suggest that this effect could have arisen from the fully thawed debris layer readily storing excess water produced in this period and mobilization of fines impinging on hydrological efficacy, with a consequent net reduction in throughflow evidenced by gradual increases in all K-values. The drainage of meltwater continued for ~45 days after nighttime T_a dropped to freezing, with around 7% of the observed runoff volume being delivered in this late and post-monsoon period. This protracted drainage corresponds well to the delay in runoff thought to relate to hysteresis caused by a deep groundwater system in the Nepal Himalaya (Andermann et al., 2012). Our data suggest that widespread supraglacial debris layers themselves may contribute to the observations of reservoir behavior in glacierized catchments at a seasonal time scale and extend the duration of glacier meltwater delivery to downstream environments.

5. Conclusions

We have demonstrated that the evolving system of supraglacial ponds and accompanying debris has the capacity to act as a fundamental modulator of proglacial discharge regimes at Khumbu Glacier. Although there is uncertainty in the causal associations between glacier surface gradient, debris cover and pond occurrence (Salerno et al., 2017), supraglacial ponds are reported to be increasingly prevalent on debris-covered glaciers and represent an active and dynamic hydrological system (Miles, Willis, et al., 2017; Miles, Steiner, et al., 2017; Narama et al., 2017; Watson et al., 2016; Watson, Quincey, Carrivick, Smith, Rowan, et al., 2017). Recently, there has been growing recognition that small changes in hydrological function in mountain regions can have substantial impacts on freshwater availability (e.g., Pritchard, 2017) and biodiversity (Jacobsen et al., 2012), and on terrestrial water bodies and ecosystems in the Himalaya (Salerno et al., 2016; Xu et al., 2009). To understand the hydrological response of debris-covered glaciers and to forecast changes in water resources and ecosystem services in the region, it is crucial to explicitly incorporate processes relating to the thermodynamics and hydrology of widespread debris mantles that can now be considered as cryotic, thermokarstic active layers—systems that are more commonly described solely in periglacial settings (Bonnaventure & Lamoureux, 2013). Further geophysical and hydrochemical exploration of debris cover (e.g., McCarthy et al., 2017; Muir et al., 2011) is needed to better define the nature of the supraglacial debris-covered drainage system and the modes and thermodynamics of hydraulic connectivity between ponds. With ~75 to 90% glacier area in the Himalaya above 4,500–5,000 m asl, the elevation range commonly associated with the regional permafrost limit (Schmid et al., 2015), the processes we describe here should be widely applicable throughout the region and highlight the important role that debris-layer supraglacial hydrology may have on mediating glacier runoff characteristics in High Mountain Asia. Long-term increases in areal extent of debris cover and ponds will not only contribute to more rapid glacier mass loss but, we propose, also alter patterns of meltwater supply and quality to downstream catchments through their roles as temporary reservoirs and flow regulators. A more complete understanding of this buffering process is crucial to improving projections of the region's future water resources in a changing climate.

Acknowledgments
All authors acknowledge the Royal Society (research grant: RG120393) and the British Society for Geomorphology (BSG). Summit Treks provided logistical support in Nepal. Patrick Wagnon kindly provided incident radiation and precipitation data. T.D.I., P.R.P., N.F.G., and J.W.B. led the analysis, writing, and conceptual development. T.D.I., A.V.R., D.J.Q., and M.J.G. undertook fieldwork in Nepal. P.R.P. provided fieldwork equipment and instruments. C.S.W. acquired and processed supraglacial lake data. All authors contributed to development, editing, and revision of the final manuscript. We thank the two reviewers who both provided insightful suggestions to help improve the paper. All new data presented here are available via www.pangaea.de: doi.org/10.1594/PANGAEA.883071 and doi.org/10.1594/PANGAEA.883419.

References

Andermann, C., Longuevergne, L., Bonnet, S., Crave, A., Davy, P., & Gloaguen, R. (2012). Impact of transient groundwater storage on the discharge of Himalayan rivers. *Nature Geoscience*, *5*(2), 127–132. https://doi.org/10.1038/ngeo1356

Bajracharya, S. R., Maharjan, S. B., Shrestha, F., Guo, W., Liu, S., Immerzeel, W., & Shrestha, B. (2015). The glaciers of the Hindu Kush Himalayas: Current status and observed changes from the 1980s to 2010. *International Journal of Water Resources Development*, *31*(2), 161–173. https://doi.org/10.1080/07900627.2015.1005731

Basnett, S., Kulkarni, A. V., & Bolch, T. (2013). The influence of debris cover and glacial lakes on the recession of glaciers in Sikkim Himalaya, India. *Journal of Glaciology*, *59*(218), 1035–1046. https://doi.org/10.3189/2013JoG12J184

Benn, D. I., Bolch, T., Hands, K., Gulley, J., Luckman, A., Nicholson, L. I., … Wiseman, S. (2012). Response of debris-covered glaciers in the Mount Everest region to recent warming, and implications for outburst flood hazards. *Earth-Science Reviews*, *114*(1-2), 156–174. https://doi.org/10.1016/j.earscirev.2012.03.008

Benn, D. I., Wiseman, S., & Hands, K. A. (2001). Growth and drainage of supraglacial lakes on debris mantled Ngozumpa Glacier, Khumbu Himal, Nepal. *Journal of Glaciology*, *47*(159), 626–638. https://doi.org/10.3189/172756501781831729

Bhatt, M. P., Takeuchi, N., & Acevedo, M. F. (2016). Chemistry of supraglacial ponds in the debris-covered area of Lirung Glacier in Central Nepal Himalayas. *Aquatic Geochemistry*, *22*(1), 35–64. https://doi.org/10.1007/s10498-015-9276-9

Bolch, T., Buchroithner, M., Pieczonka, T., & Kunert, A. (2008). Planimetric and volumetric glacier changes in the Khumbu Himal, Nepal, since 1962 using Corona, Landsat TM and ASTER data. *Journal of Glaciology*, *54*(187), 592–600. https://doi.org/10.3189/002214308786570782

Bolch, T., Kulkarni, A., Kääb, A., Huggel, C., Paul, F., Cogley, J. G., … Bajracharya, S. (2012). The state and fate of Himalayan glaciers. *Science*, *336*(6079), 310–314. https://doi.org/10.1126/science.1215828

Bonnaventure, P. P., & Lamoureux, S. F. (2013). The active layer: A conceptual review of monitoring, modelling techniques and changes in a warming climate. *Progress in Physical Geography*, *37*(3), 352–376. https://doi.org/10.1177/0309133313478314

Bookhagen, B., & Burbank, D. W. (2010). Toward a complete Himalayan hydrological budget: Spatiotemporal distribution of snowmelt and rainfall and their impact on river discharge. *Journal of Geophysical Research*, *115*, F03019. https://doi.org/10.1029/2009JF001426

Brun, F., Berthier, E., Wagnon, P., Kääb, A., & Treichler, D. (2017). A spatially resolved estimate of High Mountain Asia glacier mass balances from 2000 to 2016. *Nature Geoscience*, *10*(9), 668–673. https://doi.org/10.1038/ngeo2999

Brun, F., Buri, P., Miles, E. S., Wagnon, P., Steiner, J., Berthier, E., … Pellicciotti, F. (2016). Quantifying volume loss from ice cliffs on debris-covered glaciers using high-resolution terrestrial and aerial photogrammetry. *Journal of Glaciology*, *62*(234), 684–695. https://doi.org/10.1017/jog.2016.54

Carenzo, M., Pellicciotti, F., Mabillard, J., Reid, T., & Brock, B. W. (2016). An enhanced temperature index model for debris-covered glaciers accounting for thickness effect. *Advances in Water Resources*, *94*, 457–469. https://doi.org/10.1016/j.advwatres.2016.05.001

Di Baldassarre, G., & Montanari, A. (2009). Uncertainty in river discharge observations: A quantitative analysis. *Hydrology and Earth System Sciences*, *13*(6), 913–921. https://doi.org/10.5194/hess-13-913-2009

Evatt, G. W., Abrahams, I. D., Heil, M., Mayer, C., Kingslake, J., Mithcel, S. L., … Clark, C. D. (2015). Glacial melt under a porous debris layer. *Journal of Glaciology*, *61*(229), 825–836. https://doi.org/10.3189/2015JoG14J235

Fujita, K., & Sakai, A. (2014). Modelling runoff from a Himalayan debris-covered glacier. *Hydrology and Earth System Sciences*, *18*(7), 2679–2694. https://doi.org/10.5194/hess-18-2679-2014

Gades, A., Conway, H., Nereson, N., Naito, N., & Kadota, T. (2000). Radio echo-sounding through supraglacial debris on Lirung and Khumbu Glaciers, Nepal Himalayas. *IAHS Publication*, *264*, 13–24.

Gardelle, J., Arnaud, Y., & Berthier, E. (2011). Contrasted evolution of glacial lakes along the Hindu Kush Himalaya mountain range between 1990 and 2009. *Global and Planetary Change*, *75*(1-2), 47–55. https://doi.org/10.1016/j.gloplacha.2010.10.003

Gulley, J., & Benn, D. I. (2007). Structural control of englacial drainage systems in Himalayan debris-covered glaciers. *Journal of Glaciology*, *53*(182), 399–412. https://doi.org/10.3189/002214307783258378

Gulley, J. D., Benn, D. I., Müller, D., & Luckman, A. (2009). A cut-and-closure origin for englacial conduits in uncrevassed regions of polythermal glaciers. *Journal of Glaciology*, *55*(189), 66–80. https://doi.org/10.3189/002214309788608930

Gurnell, A. M. (1993). How many reservoirs? An analysis of flow recessions from a glacier basin. *Journal of Glaciology*, *39*, 132–134.

Hannah, D. M., Smith, B. P., Gurnell, A. M., & McGregor, G. R. (2000). An approach to hydrograph classification. *Hydrological Processes*, *14*(2), 317–338. https://doi.org/10.1002/(SICI)1099-1085(20000215)14:2%3C317::AID-HYP929%3E3.0.CO;2-T

Herschy, R. W. (1995). *Streamflow measurement*. Boca Raton, FL: CRC Press.

Hodgkins, R., Cooper, R., Tranter, M., & Wadham, J. (2013). Drainage system development in consecutive melt seasons at a polythermal, Arctic glacier, evaluated by flow recession analysis and linear reservoir simulation. *Water Resources Research*, *49*, 4230–4243. https://doi.org/10.1002/wrcr.20257

Hudson, R., & Fraser, J. (2005). The mass balance (or dry injection) method. *Streamline Watershed Management. Bulletin*, *9*, 6–12.

Immerzeel, W. W., & Bierkens, M. F. P. (2012). Asia's water balance. *Nature Geoscience*, *5*(12), 841–842. https://doi.org/10.1038/ngeo1643

Immerzeel, W. W., Van Beek, L. P. H., & Bierkens, M. F. P. (2010). Climate change will affect the Asian water towers. *Science*, *328*(5984), 1382–1385. https://doi.org/10.1126/science.1183188

Immerzeel, W. W., Van Beek, L. P. H., Konz, M., Shrestha, A. B., & Bierkens, M. F. P. (2012). Hydrological response to climate change in a glacierized catchment in the Himalayas. *Climatic Change*, *110*(3-4), 721–736. https://doi.org/10.1007/s10584-011-0143-4

Jacobsen, D., Milner, A. M., Brown, L. E., & Dangles, O. (2012). Biodiversity under threat in glacier-fed river systems. *Nature Climate Change*, *2*(5), 361–364. https://doi.org/10.1038/nclimate1435

Jobard, S., & Dzikowski, M. (2006). Evolution of glacial flow and drainage during the ablation season. *Journal of Hydrology*, *330*(3-4), 663–671. https://doi.org/10.1016/j.jhydrol.2006.04.031

Kääb, A., Berthier, E., Nuth, C., Gardelle, J., & Arnaud, Y. (2012). Contrasting patterns of early twenty-first-century glacier mass change in the Himalayas. *Nature*, *488*(7412), 495–498. https://doi.org/10.1038/nature11324

King, O., Quincey, D. J., Carrivick, J. L., & Rowan, A. V. (2017). Spatial variability in mass loss of glaciers in the Everest region, central Himalayas, between 2000 and 2015. *The Cryosphere*, *11*(1), 407–426. https://doi.org/10.5194/tc-11-407-2017

Kirkbride, M. P. (1993). The temporal significance of transitions from melting to calving termini at glaciers in the central Southern Alps of New Zealand. *The Holocene*, *3*(3), 232–240. https://doi.org/10.1177/095968369300300305

Lang, H. (1973). Variations in the relation between glacier discharge and meteorological elements. *IAHS Publication*, *95*, 85–96.

Lutz, A. F., Immerzeel, W. W., Shrestha, A. B., & Bierkens, M. F. P. (2014). Consistent increase in High Asia's runoff due to increasing glacier melt and precipitation. *Nature Climate Change*, *4*(7), 587–592. https://doi.org/10.1038/nclimate2237

Mae, S., Wushiki, H., Ageta, Y., & Higuchi, K. (1975). Thermal drilling and temperature measurements in Khumbu Glacier, Nepal Himalayas. *Seppyo*, *37*, 161–169.

McCarthy, M., Pritchard, H., Willis, I., & King, E. (2017). Ground-penetrating radar measurements of debris thickness on Lirung Glacier, Nepal. *Journal of Glaciology*, *63*(239), 543–555. https://doi.org/10.1017/jog.2017.18

Mertes, J. R., Thompson, S. S., Booth, A. D., Gulley, J. D., & Benn, D. I. (2017). A conceptual model of supra-glacial lake formation on debris-covered glaciers based on GPR facies analysis. *Earth Surface Processes and Landforms*, *42*(6), 903–914. https://doi.org/10.1002/esp.4068

Miles, E. S., Pellicciotti, F., Willis, I. C., Steiner, J. F., Buri, P., & Arnold, N. S. (2016). Refined energy-balance modelling of a supraglacial pond, Langtang Khola, Nepal. *Annals of Glaciology*, *57*(71), 29–40. https://doi.org/10.3189/2016AoG71A421

Miles, E. S., Steiner, J., Willis, I., Buri, P., Immerzeel, W. W., Chesnokova, A., & Pellicciotti, F. (2017). Pond dynamics and supraglacial-englacial connectivity on debris-covered Lirung Glacier, Nepal. *Frontiers in Earth Science*, *5*, 69.

Miles, E. S., Willis, I. C., Arnold, N. S., Steiner, J., & Pellicciotti, F. (2017). Spatial, seasonal and interannual variability of supraglacial ponds in the Langtang Valley of Nepal, 1999–2013. *Journal of Glaciology*, *63*(237), 88–105. https://doi.org/10.1017/jog.2016.120

Montaldo, N., Mancini, M., & Rosso, R. (2004). Flood hydrograph attenuation induced by a reservoir system: Analysis with a distributed rainfall-runoff model. *Hydrological Processes*, *18*(3), 545–563. https://doi.org/10.1002/hyp.1337

Muir, D. L., Hayashi, M., & McClymont, A. F. (2011). Hydrological storage and transmission characteristics of an alpine talus. *Hydrological Processes*, *25*, 2954–2966.

Narama, C., Daiyrov, M., Tadono, T., Yamamoto, M., Kääb, A., Morita, R., & Ukita, J. (2017). Seasonal drainage of supraglacial lakes on debris-covered glaciers in the Tien Shan Mountains, Central Asia. *Geomorphology*, *286*, 133–142. https://doi.org/10.1016/j.geomorph.2017.03.002

Nuimura, T., Fujita, K., Fukui, K., Asahi, K., Aryal, R., & Ageta, Y. (2011). Temporal changes in elevation of the debris-covered ablation area of Khumbu Glacier in the Nepal Himalaya since 1978. *Arctic, Antarctic, and Alpine Research*, *43*(2), 246–255. https://doi.org/10.1657/1938-4246-43.2.246

Østrem, G. (1959). Ice melting under a thin layer of moraine, and the existence of ice cores in moraine ridges. *Geografiska Annaler*, *41*(4), 228–230. https://doi.org/10.1080/20014422.1959.11907953

Parriaux, A., & Nicoud, G. F. (1990). Hydrological behaviour of glacial deposits in mountainous areas. *IAHS Publication*, *190*, 291–312.

Pritchard, H. D. (2017). Asia's glaciers are a regionally important buffer against drought. *Nature*, *545*(7653), 169–174. https://doi.org/10.1038/nature22062

Quincey, D. J., Richardson, S. D., Luckman, A., Lucas, R. M., Reynolds, J. M., Hambrey, M. J., & Glasser, N. F. (2007). Early recognition of glacial lake hazards in the Himalaya using remote sensing datasets. *Global and Planetary Change*, *56*(1-2), 137–152. https://doi.org/10.1016/j.gloplacha.2006.07.013

Ragettli, S., Pellicciotti, F., Immerzeel, W. W., Miles, E. S., Petersen, L., Heynen, M., … Shrestha, A. (2015). Unraveling the hydrology of a Himalayan catchment through integration of high resolution in situ data and remote sensing with an advanced simulation model. *Advances in Water Resources*, *78*, 94–111. https://doi.org/10.1016/j.advwatres.2015.01.013

Rantz, S.E., et al. (1982). Measurement and computation of streamflow: Volume 2. Computation of discharge. USGS Water Supply Paper 2175. USGPO (pp. 285–631).

Reynolds, J. M. (2000). On the formation of supraglacial lakes on debris-covered glaciers. *IAHS Publication*, *264*, 153–164.

Richards, K., Sharp, M., Arnold, N., Gurnell, A., Clark, M., Tranter, M., … Lawson, W. (1996). An integrated approach to modelling hydrology and water quality in glacierized catchments. *Hydrological Processes*, *10*(4), 479–508. https://doi.org/10.1002/(SICI)1099-1085(199604)10:4%3C479::AID-HYP406%3E3.0.CO;2-D

Rowan, A. V., Egholm, D. L., Quincey, D. J., & Glasser, N. F. (2015). Modelling the feedbacks between mass balance, ice flow and debris transport to predict the response to climate change of debris-covered glaciers in the Himalaya. *Earth and Planetary Science Letters*, *430*, 427–438. https://doi.org/10.1016/j.epsl.2015.09.004

Sakai, A., Fujita, K., Aoki, T., Asahi, K., & Nakawo, M. (1997). Water discharge from the Lirung Glacier in Langtang Valley, Nepal Himalayas, 1996. *Bulletin of Glacier Research*, *15*, 79–83.

Sakai, A., Nakawo, M., & Fujita, K. (2002). Distribution characteristics and energy balance of ice cliffs on debris-covered glaciers, Nepal Himalaya. *Arctic, Antarctic, and Alpine Research*, *34*(1), 12–19. https://doi.org/10.2307/1552503

Sakai, A., Takeuchi, N., Fujita, K., & Nakawo, M. (2000). Role of supraglacial ponds in the ablation process of a debris-covered glacier in the Nepal Himalayas. *IAHS Publication*, *264*, 119–132.

Salerno, F., Rogora, M., Balestrini, R., Lami, A., Tartari, G. A., Thakuri, S., … Tartari, G. (2016). Glacier melting increases the solute concentrations of Himalayan glacial lakes. *Environmental Science & Technology*, *50*(17), 9150–9160. https://doi.org/10.1021/acs.est.6b02735

Salerno, F., Thakuri, S., Tartari, G., Nuimura, T., Sunako, S., Sakai, A., & Fujita, K. (2017). Debris-covered glacier anomaly? Morphological factors controlling changes in the mass balance, surface area, terminus position, and snow line altitude of Himalayan glaciers. *Earth and Planetary Science Letters*, *471*, 19–31. https://doi.org/10.1016/j.epsl.2017.04.039

Scherler, D., Bookhagen, B., & Strecker, M. R. (2011). Spatially variable response of Himalayan glaciers to climate change affected by debris cover. *Nature Geoscience*, *4*(3), 156–159. https://doi.org/10.1038/ngeo1068

Schmid, M. O., Baral, P., Gruber, S., Shahi, S., Shrestha, T., Stumm, D., & Wester, P. (2015). Assessment of permafrost distribution maps in the Hindu Kush Himalayan region using rock glaciers mapped in Google Earth. *The Cryosphere*, *9*(6), 2089–2099. https://doi.org/10.5194/tc-9-2089-2015

Shea, J. M., Immerzeel, W. W., Wagnon, P., Vincent, C., & Bajracharya, S. (2015). Modelling glacier change in the Everest region, Nepal Himalaya. *The Cryosphere*, *9*(3), 1105–1128. https://doi.org/10.5194/tc-9-1105-2015

Shea, J. M., Wagnon, P., Immerzeel, W. W., Biron, R., Brun, F., & Pellicciotti, F. (2015). A comparative high-altitude meteorological analysis from three catchments in the Nepalese Himalaya. *International Journal of Water Resources Development*, *31*(2), 174–200. https://doi.org/10.1080/07900627.2015.1020417

Sherpa, S. F., Wagnon, P., Brun, F., Berthier, E., Vincent, C., Lejeune, Y., … Sinisolo, A. (2017). Contrasted surface mass balances of debris-free glaciers observed between the southern and the inner parts of the Everest eegion (2007–15). *Journal of Glaciology*, *63*(240), 637–651. https://doi.org/10.1017/jog.2017.30

Soncini, A., Bocchiola, D., Confortola, G., Minora, U., Vuillermoz, E., Salerno, F., … Diolaiuti, G. (2016). Future hydrological regimes and glacier cover in the Everest region: The case study of the upper Dudh Koshi basin. *Science of the Total Environment*, *565*, 1084–1101. https://doi.org/10.1016/j.scitotenv.2016.05.138

Steiner, J. F., & Pellicciotti, F. (2016). Variability of air temperature over a debris-covered glacier in the Nepalese Himalaya. *Annals of Glaciology*, *57*(71), 295–307. https://doi.org/10.3189/2016AoG71A066

Swift, D. A., Nienow, P. W., Hoey, T. B., & Mair, D. W. (2005). Seasonal evolution of runoff from Haut Glacier d'Arolla, Switzerland and implications for glacial geomorphic processes. *Journal of Hydrology*, *309*(1-4), 133–148. https://doi.org/10.1016/j.jhydrol.2004.11.016

Takeuchi, N., Sakai, A., Shiro, K., Fujita, K., & Masayoshi, N. (2012). Variation in suspended sediment concentration of supraglacial lakes on debris-covered area of the Lirung Glacier in the Nepal Himalayas. *Global Environmental Reseach*, *16*, 95–104.

Thakuri, S., Salerno, F., Smiraglia, C., Bolch, T., D'Agata, C., Viviano, G., & Tartari, G. (2014). Tracing glacier changes since the 1960s on the south slope of Mt. Everest (central Southern Himalaya) using optical satellite imagery. *The Cryosphere*, *8*(4), 1297–1315. https://doi.org/10.5194/tc-8-1297-2014

Thayyen, R. J., Gergan, J. T., & Dobhal, D. P. (2005). Monsoonal control on glacier discharge and hydrograph characteristics, a case study of Dokriani Glacier, Garhwal Himalaya, India. *Journal of Hydrology*, *306*(1-4), 37–49. https://doi.org/10.1016/j.jhydrol.2004.08.034

Thompson, S., Benn, D. I., Mertes, J., & Luckman, A. (2016). Stagnation and mass loss on a Himalayan debris-covered glacier: Processes, patterns and rates. *Journal of Glaciology*, *62*, 67–485.

Verbunt, M., Gurtz, J., Jasper, K., Lang, H., Warmerdam, P., & Zappa, M. (2003). The hydrological role of snow and glaciers in alpine river basins and their distributed modeling. *Journal of Hydrology*, *282*(1–4), 36–55. https://doi.org/10.1016/S0022-1694(03)00251-8

Vincent, C., Wagnon, P., Shea, J. M., Immerzeel, W. W., Kraaijenbrink, P., Shrestha, D., … Sherpa, S. F. (2016). Reduced melt on debris-covered glaciers: Investigations from Changri Nup Glacier, Nepal. *The Cryosphere*, *10*(4), 1845–1858. https://doi.org/10.5194/tc-10-1845-2016

Watson, C. S., Quincey, D. J., Carrivick, J. L., & Smith, M. W. (2017). Ice cliff dynamics in the Everest region of the central Himalaya. *Geomorphology*, *278*, 238–251. https://doi.org/10.1016/j.geomorph.2016.11.017

Watson, C. S., Quincey, D. J., Carrivick, J. L., Smith, M. W., Rowan, A. V., & Richardson, R. (2017). Heterogeneous water storage and thermal regime of supraglacial ponds on debris-covered glaciers. *Earth Surface Processes and Landforms*. https://doi.org/10.1002/esp.4236

Watson, S. C., Quincey, D. J., Carrivick, J. L., & Smith, M. W. (2016). The dynamics of supraglacial water storage in the Everest region, central Himalaya. *Global and Planetary Change*, *142*, 14–27. https://doi.org/10.1016/j.gloplacha.2016.04.008

Wessels, R. L., Kargel, J. S., & Kieffer, H. H. (2002). ASTER measurement of supraglacial lakes in the Mount Everest region of the Himalaya. *Annals of Glaciology*, *34*, 399–408. https://doi.org/10.3189/172756402781817545

Woo, M. K., & Steer, P. (1983). Slope hydrology as influenced by thawing of the active layer, resolute, NWT. *Canadian Journal of Earth Sciences*, *20*(6), 978–986. https://doi.org/10.1139/e83-087

Woo, M. K., & Xia, Z. (1995). Suprapermafrost groundwater seepage in gravelly terrain, resolute, NWT, Canada. *Permafrost and Periglacial Processes*, *6*(1), 57–72. https://doi.org/10.1002/ppp.3430060107

Xu, J., Grumbine, R. E., Shrestha, A., Eriksson, M., Yang, X., Wang, Y., & Wilkes, A. (2009). The melting Himalayas: Cascading effects of climate change on water, biodiversity, and livelihoods. *Conservation Biology*, *23*(3), 520–530. https://doi.org/10.1111/j.1523-1739.2009.01237.x